

FCR: Investigating Generative AI models for Forensic Craniofacial Reconstruction

Ravi Shankar Prasad^{1*} and Dinesh Singh^{2†}

^{1,2}Visual Intelligence and Machine Learning (VIML) Group, School of Computing and Electrical Engineering, Indian Institute of Technology, Mandi, 175005, Himachal Pradesh, India.

*Corresponding author(s). E-mail(s): d23033@students.iitmandi.ac.in;

Contributing authors: dineshsingh@iitmandi.ac.in;

†These authors contributed equally to this work.

Abstract

Craniofacial reconstruction in forensics is one of the processes to identify victims of crime and natural disasters. Identifying an individual from their remains plays a crucial role when all other identification methods fail. Traditional methods for this task, such as clay-based craniofacial reconstruction, require expert domain knowledge and are a time-consuming process. At the same time, other probabilistic generative models like the statistical shape model or the Basel face model fail to capture the skull and face cross-domain attributes. Looking at these limitations, we propose a generic framework for craniofacial reconstruction from 2D X-ray images. Here, we used various generative models (i.e., CycleGANs, cGANs, etc) and fine-tune the generator and discriminator parts to generate more realistic images in two distinct domains, which are the skull and face of an individual. This is the first time where 2D X-rays are being used as a representation of the skull by generative models for craniofacial reconstruction. We have evaluated the quality of generated faces using FID, IS, and SSIM scores. Finally, we have proposed a retrieval framework where the query is the generated face image and the gallery is the database of real faces. By experimental results, we have found that this can be an effective tool for forensic science.

Keywords: Forensic Craniofacial Reconstruction (FCR), Generative Models, Image retrieval

1 Introduction

Craniofacial reconstruction aims to identify individuals based on the structure of their underlying skulls. This technique is not only utilised in the field of forensics but also in various fields, including history, anthropology, and archaeology. This method is also helpful in forensic cases, such as identifying terrorists and victims of large landslides in mountainous regions or tsunamis in coastal areas. When an unidentified skull is found

at a crime scene or during a natural disaster, the forensic team tries to find the identity of the deceased individual. But, the identification is difficult when other means of identification are not possible (e.g., soft tissue, hair strands) because over time, soft tissue and hair strand decomposes. To identify the individual based on the DNA is also very difficult because the forensic team does not know with whom they have to match the DNA samples. Then, at the last, the forensic

team tries to reconstruct the face by applying clay over the skull. After reconstructing the face from the given skull, they compare this reconstructed face with a database of facial images of missing persons to identify the individual. However, this method is time-consuming and requires an artist with expert knowledge in anthropology. In the tra-

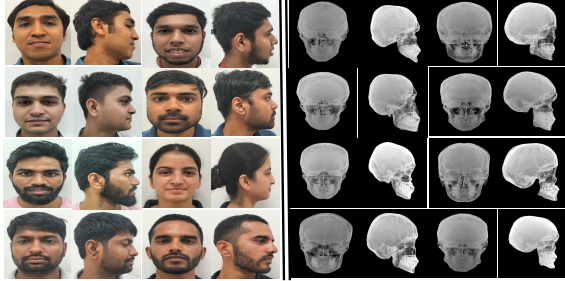


Fig. 1 Sample images from the *S2F* dataset, show paired images of face and skull from front and lateral side, respectively.

ditional method of craniofacial reconstruction, a moldable material is superimposed by hand onto an unidentified skull based on the soft tissue information (Hwang et al., 2012) and other anatomical data. The detailed study by Wilkinson (2010) shows that this process is highly subjective and requires a significant amount of creative interpretation, which can sometimes lead to unpredictable results.

To overcome the problem faced by traditional method, computerized automatic methods have been developed for skull-face overlay. There are primarily two main methods used in computer-aided craniofacial identification process. The first method is craniofacial superimposition (Campomanes-Alvarez et al., 2014; Damas et al., 2011), which directly superimposes a 2D image of the skull onto an image of the face. In the second method (Claes et al., 2010), reconstruction and editing of the face are done using a 3D statistical shape model (Dai, Pears, Smith, & Duncan, 2020). However, processing 3D skull and face data is not a trivial task, as it involves several scans at various depths and takes higher time and computational costs. Hence, to solve this problem, we used the 2D X-ray scans of the face, which are easier to obtain compared to the 3D CT image and leading to faster results and

reduced cost. Advances in machine learning and deep learning models, particularly in the field of generative models like GANs (I. Goodfellow et al., 2020), have made the task of image generation more popular. Various improved versions of GANs (Park, Efros, Zhang, & Zhu, 2020; Zhu, Park, Isola, & Efros, 2017) have introduced significant improvements in image translation. But, this image translation is done in publicly available dataset (i.e., converting horse image to zebra image or converting cat image to dog image). Hence, we propose a craniofacial reconstruction based on GenAI to synthesise craniofacial images from 2D X-ray scans of the face. This approach can be redefined as an image-to-image translation task, to generate corresponding facial images from 2D skull images. Our approach has two main advantages. First, it effectively captures the complex relationship between the skull and the face. Second, unlike CT scans, it does not require data from scans of the entire head, as it only uses frontal and lateral views from facial X-ray scans.

The major contributions of this research are as follows;

- We have proposed a generative framework for 2D craniofacial reconstruction using generative AI.
- We have also extended the benchmark *S2F* dataset for this purpose. The details of the dataset are given in section 3. Figure 1 shows a sample of the dataset.
- We conducted extensive experiments and comparative analysis on various generative models (i.e., CycleGANs, cGANs) for cross-domain craniofacial reconstruction and evaluated the quality of generated face images using FID, IS and SSIM scores.
- We also evaluated the performance of different deep models (i.e., ResNet, VGG16, DenseNet) on face retrieval tasks.

2 Related work

Craniofacial reconstruction. A few attempts have been made in craniofacial reconstruction (CR) and matching the crano (i.e., skull), to the face. Tradition methods, (Hwang et al., 2012; Wilkinson, 2010) describes how soft tissue information is used for reconstructing a face from

the given skull. Apart from manual intervention and expert dependency, these methods also have limited scalability, lack generalisation across populations, and possess limited ground truth validation. In classical machine learning methods, there have been a few works conducted for CR, such as least squares support vector regression (Li, Chang, Qiao, Liu, & Duan, 2014), latent root regression (Berar, Tilotta, Glaunès, & Rozenholc, 2011), and partial least squares regression Jia et al. (2021). However, these methods struggle with limited data, often miss local facial details, and depend heavily on accurate landmarks. These limitations highlight the necessity for more adaptable, data-driven deep learning methods that effectively capture complex patterns in craniofacial data. As the primary goal of CR is to identify the individual by reconstructing its face. However to learn cross-domain identity representation to identify individuals from the X-ray scans (i.e., skull), Prasad and Singh (2025) match to gallery face images and identify which person's skull it is. But, due to the large gap between the two modalities, which is the skull and face, models are overburdened with the responsibility of aligning the two modalities. Hence, our approach tackles this problem by converting the skull image into a face image and then matching the images in a similar domain and modalities. Also, the reconstruction can be used for the identification of individuals by humans.

Generative AI. With the advancement of deep models and generative artificial intelligence (GenAI), the task of generating images has become very popular. Generative adversarial networks (GANs) have achieved remarkable success in generating images in unpaired image-to-image translation tasks, particularly with the introduction of CycleGAN (Zhu, Park, et al., 2017). CycleGAN eliminates the need for paired data by enforcing cycle consistency loss, allowing effective domain translation between two unaligned datasets. (Li et al., 2022) describes how GANs can be used for craniofacial reconstruction. However, this work utilises a CT scan dataset, which is more challenging to obtain than X-ray scans. We have also observed that these GenAI models often struggle to preserve fine-grained semantic information across domains, particularly in tasks

involving structural complexity, such as skull-to-face synthesis. To address this issue, the patch-wise contrastive loss, proposed in (Park et al., 2020), enforces consistency in patch-wise semantic relations between the input and generated output. We utilise an adversarial loss function to learn the mapping between the source and target domains, ensuring that the translated images closely resemble those from the target domain. This technique enhances the model's ability to produce high-quality, indistinguishable image translations. In our work, we have employed multiple methods inspired by these papers; however, instead of utilising generic and CT scan datasets, we have used a benchmark *S2F* dataset. Also, the previous models computed only the FID scores (Jayasumana et al., 2024) as a generative evaluation metric; we have included Inception Score (IS) (Barratt & Sharma, 2018) and Structural Similarity Index scores (SSIM) (Nilsson & Akenine-Möller, 2020) as quantitative metrics to evaluate our generated images.

Image translation and cycle-consistency.

Basically, image translation means converting an image from one domain into another domain. Image translation and cycle consistency play a crucial role in paired image-to-image translation (Isola, Zhu, Zhou, & Efros, 2017), which maps images from an input domain to an output domain using adversarial loss (I.J. Goodfellow et al., 2014), alongside a reconstruction loss that measures the difference between the generated result and the target. In unpaired translation settings, where corresponding examples from the domains are not available, cycle consistency has emerged as the standard method for enforcing correspondence (Kim, Cha, Kim, Lee, & Kim, 2017; Yi, Zhang, Tan, & Gong, 2017; Zhu, Park, et al., 2017). This technique involves learning an inverse mapping from the output domain back to the input and verifying if the original input can be accurately reconstructed. Alternatives like UNIT (Liu, Breuel, & Kautz, 2017) and MUNIT (X. Huang, Liu, Belongie, & Kautz, 2018) propose learning a shared intermediate "content" latent space. Recent research has expanded these methods to handle multiple domains and multi-modal synthesis (Almahairi, Rajeshwar, Sordoni, Bachman, & Courville, 2018; Choi et al., 2018; Lee, Tseng, Huang, Singh, & Yang, 2018; Liu et

al., 2019; Zhu, Zhang, et al., 2017), while also enhancing the quality of the results (Gokaslan, Ramanujan, Ritchie, Kim, & Tompkin, 2018; Liang, Zhang, Lin, & Xing, 2018; Tang, Xu, Sebe, & Yan, 2019; Wu, Cao, Li, Qian, & Loy, 2019; Zhang, Pfister, & Li, 2019). In all these instances, cycle consistency is utilized in various ways: (a) between two image domains, (b) mapping from images to latent representations, and (c) mapping from latent representations back to images.

Although effective, the underlying bijective assumption associated with cycle consistency can sometimes be overly restrictive. Achieving perfect reconstruction is particularly challenging, especially when images from one domain possess additional information that is not available in the other domain. However, no work has been done in craniofacial reconstruction, including 2D X-ray face images.

3 Dataset

We have used the *S2F* dataset (Prasad & Singh, 2025) and extended the dataset samples from 40 individuals to 51 individuals following the same dataset creation procedures. As we know, training deep models effectively requires a large number of labelled datasets, but obtaining paired data of faces and skulls at a large scale is a challenging task. To address this challenge, X-ray scans of the individual's faces are conducted from both front and lateral views. The purpose of conducting X-ray scans is that they are an affordable and widely accessible imaging technique that provides valuable information about skull structure. Second, optical images of individuals' faces from lateral and frontal views are also taken. Finally, each scan is paired with a corresponding facial image of the volunteers who participated in the research. Fig. 1 presents some samples of the pairwise dataset. The final dataset of 51 individuals is prepared by decomposing the X-ray images of participants by removing the soft tissue portions so that only the hard tissue remains.

In the *S2F* dataset, all volunteers are young adults, specifically aged between 21 and 30 years. Among the volunteers of 51 individuals, there were 22 females and 29 males. This diverse group provided valuable insights for our investigation into the relationship between X-ray imagery and facial morphology. The X-ray images were captured

using a clinical X-ray scanner system at the institute's health centre. For training these generative models, we perform four types of data augmentation (i.e., horizontal flip, rotation, colour jitter and affine) to improve the quality of unbalanced *S2F* datasets. Initially, we have 102 skull and face pairs, which include 51 lateral and 51 frontal views, respectively. The dataset is split into an 80:20 ratio for training and testing. Out of 102 pairs, 20 pairs are randomly selected for testing. For training the model, we performed the above-mentioned data augmentation on 82 training image pairs, resulting in a total of 410 pairs. By effectively increasing both the similarity of augmented data points to the original samples and introducing a wider range of diverse examples, this approach makes more balanced and comprehensive dataset.

4 Methodology

We investigate four generative models for the craniofacial reconstruction task. The first one is CycleGAN (Zhu, Park, et al., 2017), the second is Conditioned GAN (Isola et al., 2017), the third is CUT (Park et al., 2020), and the last one is FastCUT (Park et al., 2020).

4.1 X-ray soft tissue elimination

As mentioned in Section §3, we have 2D X-ray images of faces that resemble skull images. However, the X-ray images also contain the effect of soft tissue. To ensure that the X-ray images accurately represent the skull, we manually removed the soft tissue components from the 2D X-ray images. Figure 3 shows some samples of real and soft tissue eliminated X-ray images, respectively.

4.2 CycleGAN

In this section, we present our first generative model, which is CycleGAN (Zhu, Park, et al., 2017), a generative framework as shown in Figure 2 for craniofacial reconstruction using 2D X-ray images. Initially, this model learns the mapping of embeddings across domains to perform reconstruction with unsupervised settings. Here, an unsupervised setting means that during training, CycleGAN does not need paired images of skull and face to learn the translation from the skull domain to the face domain. To enable learning without paired data, CycleGAN uses cyclic

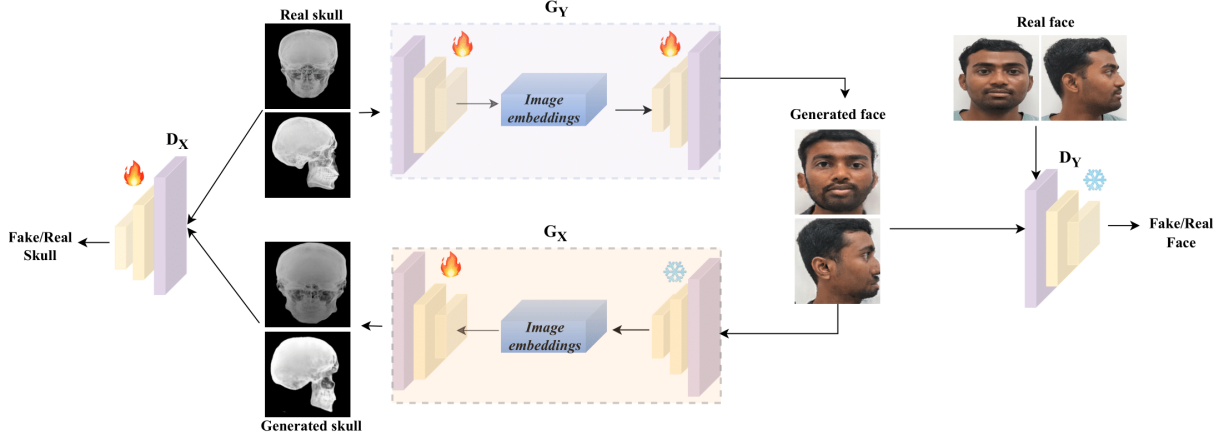


Fig. 2 Our architecture consists of two frameworks, one is X-ray soft tissue decomposition, which decomposes soft tissue from the X-ray image so that it resembles the skull, and the other consists of two Generators. Generator G_Y generates images for the first domain, which is *skull*, while generator G_X generates images for the second domain, which is *face*. This design helps to produce images that look good and fit well with their context. Using both generators allows for better image creation in each domain. The discriminator D_Y encourages the G_Y to convert inputs from domain *skull* into outputs that are indistinguishable from those in domain *face*. Conversely, discriminator D_X serves the same purpose for *face*, ensuring that generator G_X translates inputs from domain *face* into outputs that closely resemble those in domain *skull*. (Best viewed in colours)



Fig. 3 Sample soft tissue eliminated X-ray images in frontal and lateral views, respectively, where (a) is the real X-ray images and (b) is the soft tissue eliminated images.

loss in Eq. 2, which ensure that when a skull image is translated to a face image, it must come back to the source domain. Also, to preserve the appearance of the face images that are already in target domain, this model uses identity loss in Eq. 3.

Adversarial loss. In this work, we employ adversarial loss (I.J. Goodfellow et al., 2014) to promote visual similarity between our output and images from the target domain, as follows:

$$\begin{aligned} \mathcal{L}_{\text{GAN}}(G, D, X, Y) = & \mathbb{E}_{y \sim Y} [\log D(y)] \\ & + \mathbb{E}_{x \sim X} [\log(1 - D(G(x)))] \end{aligned} \quad (1)$$

Cyclic loss in CycleGAN:

$$\begin{aligned} \mathcal{L}_{\text{cycle}}(G_Y, G_X) = & \mathbb{E}_{x \sim p_{\text{data}}(x)} [\|G_X(G_Y(x)) - x\|_1] \\ & + \mathbb{E}_{y \sim p_{\text{data}}(y)} [\|G_Y(G_X(y)) - y\|_1] \end{aligned} \quad (2)$$

Identity loss in CycleGAN:

$$\begin{aligned} \mathcal{L}_{\text{identity}}(G_Y, G_X) = & \mathbb{E}_{y \sim p_{\text{data}}(y)} [\|G_Y(y) - y\|_1] \\ & + \mathbb{E}_{x \sim p_{\text{data}}(x)} [\|G_X(x) - x\|_1] \end{aligned} \quad (3)$$

Taking help from the above loss functions, we have defined cycleGAN loss as:

$$\begin{aligned} L(G_Y, G_X, D_Y, D_X) = & L_{\text{GAN}}(G_Y, D_Y, X, Y) \\ & + L_{\text{GAN}}(G_X, D_X, Y, X) \\ & + \lambda \mathcal{L}_{\text{cycle}}(G_X, G_Y) \\ & + \mathcal{L}_{\text{identity}}(G_Y, G_X) \end{aligned} \quad (4)$$

Where G_X , G_Y are generators for generating skull and face images respectively, and D_X , D_Y are discriminators for differentiating between the generated skull image and real skull and between generated face image and real face image respectively. In this craniofacial reconstruction, X is the skull and Y is the face. As shown in Fig. 2, first,

we preprocess the X-ray by eliminating the effect of soft tissue. This process takes the soft tissue present in the X-ray image and separates it in a way that highlights the underlying structures of the skull. Essentially, the goal is to make the image look more like a clear representation of the skull by removing soft tissue details.

The main framework consists of two generators, G_X and G_Y respectively. The encoder of G_Y is trainable, while we used pretrained encoder in G_X to extract the features from skull and face images. Each generator specializes in generating images within a specific domain. G_Y is trainable and responsible for producing images of faces, while G_X is also trainable and focuses on generating images of skulls. This division of generators allows the architecture to create images that are not only visually appealing but also contextually appropriate for each domain.

To enhance the image generation process, two discriminators are embedded, D_X and D_Y . D_Y 's role is to evaluate the output generated by G_Y . Its goal is to ensure that the face images produced by G_Y are so realistic and high-quality that they cannot be easily distinguished from actual face images. On the other hand, D_X works with G_X to ensure that the skulls it generates appear authentic and closely resemble real skulls.

By utilizing both generators and their corresponding discriminators, this architecture improves the quality of the images produced in each specific domain, leading to better overall image creation and a more accurate representation of both skulls and faces derived from X-ray images.

4.3 Conditioned GAN

In this second generative framework, we used Conditioned GAN [Isola et al. \(2017\)](#), also known as Pix2pix, to translate an image from the skull to the face domain. This model used a supervised setting, which means it needs paired images of the skull and their respective face to learn the mapping function. The generator in a conditioned GAN takes both a random noise vector (i.e., z) and an input image (i.e., x), and this input image guides the entire generator process. In Figure 2, if we follow only one side of translation, then it can be modelled as the framework for a conditioned GAN, because this GAN has only one generator

and one discriminator. Given below is the loss function used in the conditioned GAN:

$$\begin{aligned} \mathcal{L}_{cGAN}(G_Y, D_Y) = & \mathbb{E}_{x,y} [\log D_Y(x, y)] \\ & + \mathbb{E}_{x,z} [\log (1 - D_Y(x, G_Y(x, z)))] \end{aligned} \quad (5)$$

4.4 Learning cross-domain image representation using CUT

In this section, we used the CUT ([Park et al., 2020](#)) model, which is contrastive learning for unpaired image-to-image translation. This model is an improved version of CycleGAN in only one-sided image translation, basically consists of only one generator and one discriminator. Here, one-sided image translation means to translate an image from the skull to the face domain only, as our objective is to develop a mapping function that accurately relates the embeddings from skull features to their corresponding embeddings obtained from facial features. To accomplish this task effectively, several studies on a contrastive learning approach ([Bachman, Hjelm, & Buchwalter, 2019](#); [T. Chen, Kornblith, Norouzi, & Hinton, 2020](#); [X. Chen, Fan, Girshick, & He, 2020](#); [Park et al., 2020](#)) have been done. This methodology is designed to minimize the distance between embeddings of similar pairs, where the skull and face belong to the same individual, while maximizing the distance between embeddings of dissimilar pairs, which belong to different individuals. By doing so, we enhance the model's ability to distinguish between unique facial characteristics tied to distinct skull structures, ultimately improving the precision of our mapping function.

Patch-wise learning for craniofacial reconstruction. Fig. 4 represents patch-wise learning for cross-domain image reconstruction. Instead of only working on the whole skull image, the CUT model ([Park et al., 2020](#)) also works on the patch level. Patch-wise loss used in the CUT model maps corresponding patches in the source and target domains at a specific location. For example, the nasal patch of the skull should more closely match the nasal patch of the face than the other patches of the given input skull. Hence, to make the model learn this type of patch-wise semantic attributes, we selected L layers from the encoder part of CUT ([Park et al., 2020](#)) model, extracted the feature maps from these layers, and

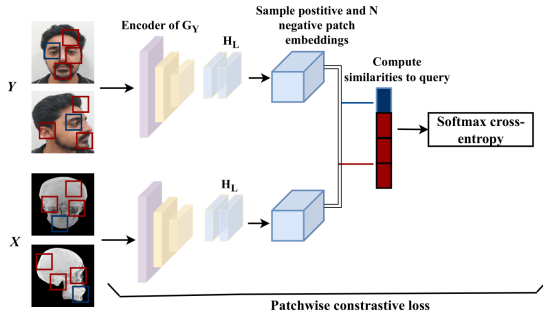


Fig. 4 First, images from both domains (X and Y) are encoded using encoders of generator G_Y and two-layer MLP networks (H_L). Then, the query patch from the output Y is sampled and compared with the input patch X at the same location, and finally, the cross-entropy loss function is used to find the patch-wise contrastive loss. (Best viewed in colors)

then passed these feature maps through a small two-layer MLP network (H_l). This MLP network produces a stack of features. Now, we have defined the stack of source (i.e., skull) features as:

$$S = \{H_l(G_{enc}^l(x))\}_{l=1}^L \quad (6)$$

In the above equation, G_{enc}^l is the output of the l -th layer of the encoder of generator G_Y where $l \in \{1, 2, \dots, L\}$ and x is the skull image patch.

In the same way, we encoded the target image (face) as:

$$F = \{H_l(G_{enc}^l(G_Y(x)))\}_{l=1}^L \quad (7)$$

Now, we have encoded the skull (x) and face (y) image patches, and for patch-wise contrastive learning, we have used cross-entropy loss, which is given as:

$$\ell(F, S^+, \{S^-\}) = -\log \left(\frac{\exp(F \cdot S^+ / \tau)}{\exp(F \cdot S^+ / \tau) + \sum_{n=1}^N \exp(F \cdot S_n^- / \tau)} \right) \quad (8)$$

Where,

- F : generated face feature $\in \mathbb{R}^K$ (K -dimensional feature vectors from output *face* patch)
- S^+ : positive key $\in \mathbb{R}^K$ (from input *skull* patch at the same location)
- S^- : negative keys $\in \mathbb{R}^{N \times K}$ (N number of negative samples from other *skull* patches)
- τ : temperature hyperparameter which is set to 0.07.

The final patch-wise loss (Park et al., 2020) for particular patch location ($s \in \{1, \dots, S_l\}$) in a feature map is given as:

$$\mathcal{L}_{\text{Patch}}(G_Y, H, X) = \mathbb{E}_{x \sim X} \left[\sum_{l=1}^L \sum_{s=1}^{S_l} \ell(F_s^l, S_s^{+l}, \{S_s^{-l}\}) \right] \quad (9)$$

Similarly, to preserve the identity of the target domain (face), generator of CUT model is provided with the input image from the target domain (i.e., face image). Hence, this process serves as a regularizer and prevent the generator from making unnecessary changes to the images that are already in the target domain (face) and for this identity loss in CUT is defined as:

$$\mathcal{L}_{\text{identity}}(G_Y, Y) = \mathbb{E}_{y \sim Y} \|G_Y(y) - y\|_1 \quad (10)$$

And the final GAN loss with patch-wise loss function is given as:

$$\begin{aligned} \mathcal{L} = \mathcal{L}_{\text{GAN}}(G_Y, D_Y, X, Y) + \lambda_X \mathcal{L}_{\text{Patch}}(G_Y, H, X) + \\ \lambda_Y \mathcal{L}_{\text{identity}}(G_Y, Y) \end{aligned} \quad (11)$$

Where X is the source domain image (i.e., skull), Y is the target domain image (i.e., face), P is the image patch and H is the feature encoder, or the layers within G , that extracts feature maps for the Patch loss (Park et al., 2020). In practice, H is implemented using selected intermediate layers of G , rather than as a separate network. λ_X and λ_Y are hyperparameters which are 1. In the Eq. 11, if we put λ_X and λ_Y equal to 10 and 0, respectively, then it can be modelled as FastCUT (Park et al., 2020).

4.5 Face recognition (FR) and image retrieval (IR) module for generated images.

In our experiments, to evaluate the effectiveness of the reconstructed faces generated by generative models, each generated face is compared to all real faces in a large database. For this, we utilise four deep models (VGG16, ResNet18, ResNet101 and DenseNet121) as a backbone to extract the features of generated images and compare them to the features of real faces in the database. A

retrieval framework is essential in forensic applications because it allows for the efficient and accurate identification of unknown individuals through similarity-based searches in large databases. There were several studies conducted for image retrieval in many different applications, as mentioned in (Yu & Kovashka, 2020; Zaeemzadeh et al., 2021; Zhao, Feng, Wu, & Yan, 2017). Figure 5 shows our proposed retrieval framework. When provided with a query image (generated face), the system retrieves the most relevant images (faces) from a gallery by matching the features of the query face image with the features of the gallery face images. In this framework, we have used four deep models (He, Zhang, Ren, & Sun, 2016; G. Huang, Liu, Van Der Maaten, & Weinberger, 2017; Salimans et al., 2016) to extract the features or embeddings of face images. Feature matching is performed by calculating the Euclidean distance between the embeddings of the query face image and the gallery face images. The face image from the gallery with the minimum distance to the query face is considered the matched face. We utilized two retrieval metrics—recall and mean average precision (mAP)—which are crucial in the field of forensics.

In forensic applications, recall and mAP are important retrieval metrics (Manning, 2009) because recall ensures that true identities are not missed, even if they do not appear as the top match, and mAP takes into account both the ranking of the results and the presence of relevant items, making it a comprehensive metric. In forensic contexts, where multiple relevant images or identities may need to be retrieved, mAP effectively captures how well the system ranks all potential matches.

5 Experiments

The primary objective of the CR task is to identify the individual's face based on the underlying unknown skull; thus, the effectiveness of reconstructed faces in recognition algorithms is essential. Hence, we tested various baselines of generative models in unpaired and paired cross-domain image translation models with the benchmark *S2F* dataset.

5.1 Training with baseline models

There are a total of four generative models used. Table 1 shows the comparative analysis of various generative models using the *S2F* dataset, and for each model, we have calculated three evaluation metrics while translating from one domain to another domain.

5.2 Experimental results

Quantitative comparison. To evaluate the performance of different generative models, we have used three evaluation metrics, Fréchet Inception Distance (FID) (Heusel, Ramsauer, Unterthiner, Nessler, & Hochreiter, 2017), Inception Score (IS) (Salimans et al., 2016), and Structural Similarity Index scores (SSIM) (Wang, Bovik, Sheikh, & Simoncelli, 2004). Table 1 provides comprehensive quantitative results on the *S2F* dataset. From this table, we can conclude that the FastCUT model, which is a lighter version of CycleGAN, is the best-performing model in the craniofacial reconstruction task. Table 2 provides a comparative analysis of evaluation metrics between different deep models for the face retrieval task, from which the DenseNet121 model gets better recall and mAP than all other deep models.

Qualitative comparison. Fig. 6 and Fig. 7 show the qualitative comparisons between different generative models from both lateral and frontal views, when translating from skull to face domain. Out of 4 models, FastCUT is outperforming all other models by preserving semantic features of the target domain with *S2F* dataset. Figure 9 shows some qualitative results on the retrieval of the top 10 gallery faces, where the correctly matched face is shown in a green border. For this retrieval, we use DenseNet121 as a backbone for feature extraction.

6 Discussion & Limitations

From this work, we have observed that generative models like GANs are very good in the image generation task, but there are several failure cases when these models fail to generate a realistic image similar to the ground truth image. Figure 8 shows several failure cases. The reason for this failure case might be due to the complex distribution of the training dataset. We also explored

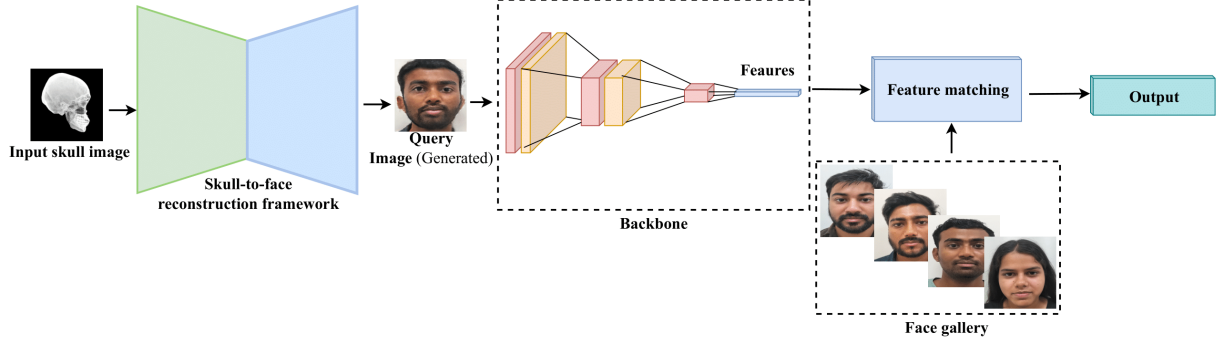


Fig. 5 Face retrieval framework for the generated query face image from the gallery face images. First, face image is reconstructed from the input skull image with reconstruction framework, then this generated face is treated as query image and then feature of query face is extracted from the backbone which consists of different pre-trained deep models and then feature matching is done between the query feature and precomputed face gallery features.

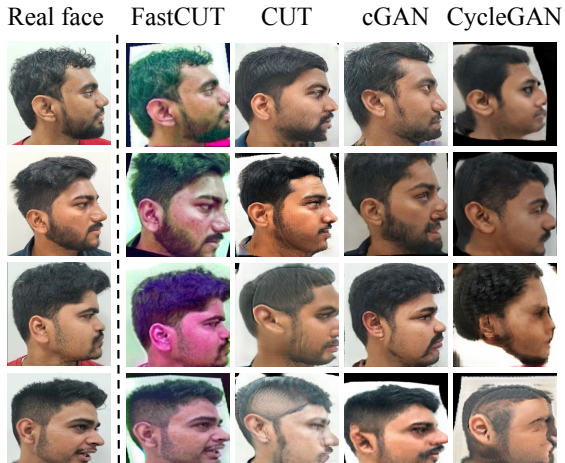


Fig. 6 Qualitative comparison, where the generated *side face* is compared with the ground truth *side face* when translating from skull to face.

that with the *S2F* dataset, the heavy architecture of some GAN models, like CycleGAN and Conditioned GAN, fails to capture the intrinsic properties of skull images.

6.1 Conclusion

This work presents an effective method for cranio-facial reconstruction using 2D frontal and lateral-view images from facial scans. We conducted experiments on 2D X-ray images because they are easier to collect. The results demonstrate that these generative techniques can be valuable in forensics, particularly when other identification

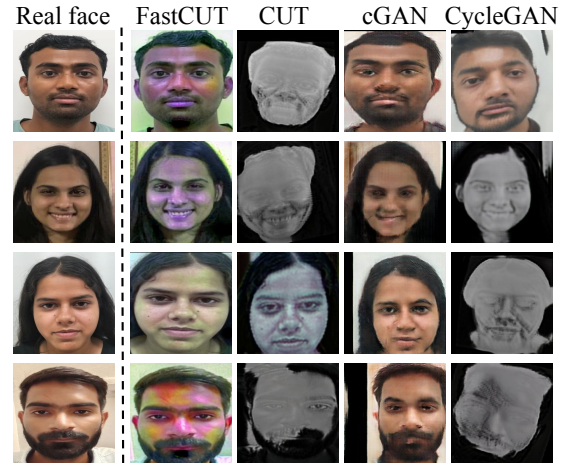


Fig. 7 Qualitative comparison, where the generated *front face* is compared with the ground truth *front face* when translating from skull to face.



Fig. 8 Failed case of CycleGAN, where (a) is the ground truth face images and (b) is the generated face, when translating an image from skull→face.

Table 1 We conduct a comparative analysis of various methods utilising the *S2F* dataset along with standard evaluation metrics.

Methods	Real skull → Generated face		
	FID↓	IS↑	SSIM↑
CycleGAN (Zhu, Park, et al., 2017)	313.46	2.48 ± 0.14	0.33
cGAN (Isola et al., 2017)	148.84	1.66 ± 0.28	0.66
CUT (Park et al., 2020)	305.04	2.67 ± 0.20	0.32
FastCUT (Park et al., 2020)	63.65	2.72 ± 0.22	0.66

Table 2 Comparison of Top-10 and Top-20 Recall and mAP for different face recognition models. The best model is marked in bold.

Models	Recall		mAP	
	Top-10	Top-20	Top-10	Top-20
VGG16 (Simonyan & Zisserman, 2014)	0.03	0.06	0.62	0.56
ResNet18 (He et al., 2016)	0.02	0.05	0.67	0.60
ResNet101 (He et al., 2016)	0.04	0.08	0.77	0.75
DenseNet121 (G. Huang et al., 2017)	0.04	0.08	0.81	0.74

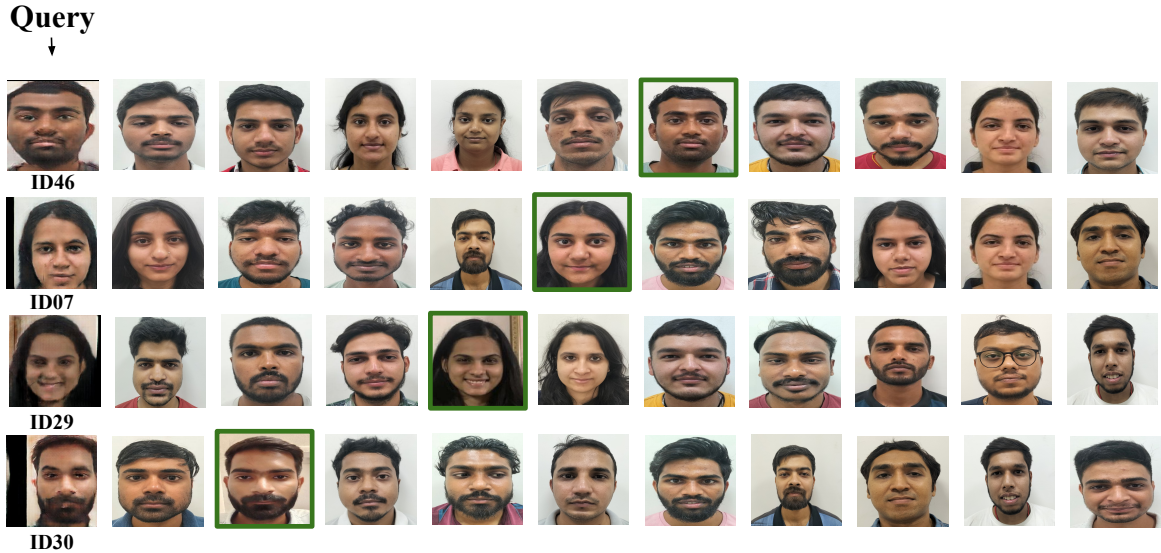


Fig. 9 Retrieval results in which the generated image is treated as the query image and gallery face image with a green border is the matched face.

methods (such as fingerprinting, dental records, radiological materials, or DNA analysis) are ineffective for human remains. Through comparative quantitative and qualitative analyses of various generative models for the skull-to-face image

translation problem, we found that the Fast-CUT model outperforms other generative models in cross-domain image translation. This model can generate realistic human faces from the provided 2D X-ray skull images. There are also some failed cases, which we need to improve. We have also conducted experiments on the face retrieval task by matching the features of the query face image (i.e., generated image) with the features of gallery face images, and we have found that out of four deep models, DenseNet121 outperforms the other models in the face retrieval problem and from these observations, we can conclude that this can be used in forensic science for person identification.

7 Acknowledgment

During the preparation of this work the author(s) used Grammarly in order to correct the spellings and grammars. After using this tool, the author(s) reviewed and edited the content as needed and take(s) full responsibility for the content of the publication. I also want to sincerely thank the volunteers who dedicated their time and effort to help create the benchmark dataset called *S2F*. I also appreciate the cooperation and assistance from the Health Centre during the data collection process.

7.1 Data availability

Our data will be made available on request.

References

- Almahairi, A., Rajeshwar, S., Sordoni, A., Bachman, P., Courville, A. (2018). Augmented cyclegan: Learning many-to-many mappings from unpaired data. *International conference on machine learning* (pp. 195–204).
- Bachman, P., Hjelm, R.D., Buchwalter, W. (2019). Learning representations by maximizing mutual information across views. *Advances in neural information processing systems*, 32, ,
- Barratt, S., & Sharma, R. (2018). A note on the inception score. *arXiv preprint arXiv:1801.01973*, ,
- Berar, M., Tilotta, F.M., Glaunès, J.A., Rozenholc, Y. (2011). Craniofacial reconstruction as a prediction problem using a latent root regression model. *Forensic science international*, 210(1-3), 228–236,
- Campomanes-Alvarez, B.R., Ibáñez, O., Navarro, F., Alemán, I., Botella, M., Damas, S., Cordón, O. (2014). Computer vision and soft computing for automatic skull–face overlay in craniofacial superimposition. *Forensic Science International*, 245, 77–86,
- Chen, T., Kornblith, S., Norouzi, M., Hinton, G. (2020). A simple framework for contrastive learning of visual representations. *International conference on machine learning* (pp. 1597–1607).
- Chen, X., Fan, H., Girshick, R., He, K. (2020). Improved baselines with momentum contrastive learning. *arXiv preprint arXiv:2003.04297*, ,
- Choi, Y., Choi, M., Kim, M., Ha, J.-W., Kim, S., Choo, J. (2018). Stargan: Unified generative adversarial networks for multi-domain image-to-image translation. *Proceedings of the ieee conference on computer vision and pattern recognition* (pp. 8789–8797).
- Claes, P., Vandermeulen, D., De Greef, S., Willems, G., Clement, J.G., Suetens, P. (2010). Computerized craniofacial reconstruction: conceptual framework and review. *Forensic science international*, 201(1-3), 138–145,
- Dai, H., Pears, N., Smith, W., Duncan, C. (2020). Statistical modeling of craniofacial shape and texture. *International Journal of Computer Vision*, 128(2), 547–571,
- Damas, S., Cordon, O., Ibanez, O., Santamaria, J., Alemán, I., Botella, M., Navarro, F.

- (2011). Forensic identification by computer-aided craniofacial superimposition: a survey. *ACM Computing Surveys (CSUR)*, 43(4), 1–27,
- Gokaslan, A., Ramanujan, V., Ritchie, D., Kim, K.I., Tompkin, J. (2018). Improving shape deformation in unsupervised image-to-image translation. *Proceedings of the european conference on computer vision (eccv)* (pp. 649–665).
- Goodfellow, I., Pouget-Abadie, J., Mirza, M., Xu, B., Warde-Farley, D., Ozair, S., ... Bengio, Y. (2020). Generative adversarial networks. *Communications of the ACM*, 63(11), 139–144,
- Goodfellow, I.J., Pouget-Abadie, J., Mirza, M., Xu, B., Warde-Farley, D., Ozair, S., ... Bengio, Y. (2014). Generative adversarial nets. *Advances in neural information processing systems*, 27, ,
- He, K., Zhang, X., Ren, S., Sun, J. (2016). Deep residual learning for image recognition. *Proceedings of the ieee conference on computer vision and pattern recognition* (pp. 770–778).
- Heusel, M., Ramsauer, H., Unterthiner, T., Nessler, B., Hochreiter, S. (2017). Gans trained by a two time-scale update rule converge to a local nash equilibrium. *Advances in neural information processing systems*, 30, ,
- Huang, G., Liu, Z., Van Der Maaten, L., Weinberger, K.Q. (2017). Densely connected convolutional networks. *Proceedings of the ieee conference on computer vision and pattern recognition* (pp. 4700–4708).
- Huang, X., Liu, M.-Y., Belongie, S., Kautz, J. (2018). Multimodal unsupervised image-to-image translation. *Proceedings of the european conference on computer vision (eccv)* (pp. 172–189).
- Hwang, H.-S., Park, M.-K., Lee, W.-J., Cho, J.-H., Kim, B.-K., Wilkinson, C.M. (2012). Facial soft tissue thickness database for craniofacial reconstruction in korean adults. *Journal of forensic sciences*, 57(6), 1442–1447,
- Isola, P., Zhu, J.-Y., Zhou, T., Efros, A.A. (2017). Image-to-image translation with conditional adversarial networks. *Proceedings of the ieee conference on computer vision and pattern recognition* (pp. 1125–1134).
- Jayasumana, S., Ramalingam, S., Veit, A., Glasner, D., Chakrabarti, A., Kumar, S. (2024). Rethinking fid: Towards a better evaluation metric for image generation. *Proceedings of the ieee/cvf conference on computer vision and pattern recognition* (pp. 9307–9315).
- Jia, B., Zhao, J., Xin, S., Duan, F., Pan, Z., Wu, Z., ... Zhou, M. (2021). Craniofacial reconstruction based on heat flow geodesic grid regression (hf-ggr) model. *Computers & Graphics*, 97, 258–267,
- Kim, T., Cha, M., Kim, H., Lee, J.K., Kim, J. (2017). Learning to discover cross-domain relations with generative adversarial networks. *International conference on machine learning* (pp. 1857–1865).
- Lee, H.-Y., Tseng, H.-Y., Huang, J.-B., Singh, M., Yang, M.-H. (2018). Diverse image-to-image translation via disentangled representations. *Proceedings of the european conference on computer vision (eccv)* (pp. 35–51).
- Li, Y., Chang, L., Qiao, X., Liu, R., Duan, F. (2014). Craniofacial reconstruction based on least square support vector regression. *2014 ieee international conference on systems, man, and cybernetics (smc)* (pp. 1147–1151).
- Li, Y., Wang, J., Liang, W., Xue, H., He, Z., Lv, J., Zhang, L. (2022). Cr-gan: Automatic craniofacial reconstruction for personal identification. *Pattern Recognition*, 124, 108400,

- Liang, X., Zhang, H., Lin, L., Xing, E. (2018). Generative semantic manipulation with mask-contrasting gan. *Proceedings of the european conference on computer vision (eccv)* (pp. 558–573).
- Liu, M.-Y., Breuel, T., Kautz, J. (2017). Unsupervised image-to-image translation networks. *Advances in neural information processing systems*, 30, ,
- Liu, M.-Y., Huang, X., Mallya, A., Karras, T., Aila, T., Lehtinen, J., Kautz, J. (2019). Few-shot unsupervised image-to-image translation. *Proceedings of the ieee/cvf international conference on computer vision* (pp. 10551–10560).
- Manning, C.D. (2009). *An introduction to information retrieval*.
- Nilsson, J., & Akenine-Möller, T. (2020). Understanding ssim. *arXiv preprint arXiv:2006.13846*, ,
- Park, T., Efros, A.A., Zhang, R., Zhu, J.-Y. (2020). Contrastive learning for unpaired image-to-image translation. *Computer vision–eccv 2020: 16th european conference, glasgow, uk, august 23–28, 2020, proceedings, part ix 16* (pp. 319–345).
- Prasad, R.S., & Singh, D. (2025). Cross-domain identity representation for skull to face matching with benchmark dataset. *arXiv preprint arXiv:2507.08329*, ,
- Salimans, T., Goodfellow, I., Zaremba, W., Cheung, V., Radford, A., Chen, X. (2016). Improved techniques for training gans. *Advances in neural information processing systems*, 29, ,
- Simonyan, K., & Zisserman, A. (2014). Very deep convolutional networks for large-scale image recognition. *arXiv preprint arXiv:1409.1556*, ,
- Tang, H., Xu, D., Sebe, N., Yan, Y. (2019). Attention-guided generative adversarial networks for unsupervised image-to-image translation. *2019 international joint conference on neural networks (ijcnn)* (pp. 1–8).
- Wang, Z., Bovik, A.C., Sheikh, H.R., Simoncelli, E.P. (2004). Image quality assessment: from error visibility to structural similarity. *IEEE transactions on image processing*, 13(4), 600–612,
- Wilkinson, C. (2010). Facial reconstruction–anatomical art or artistic anatomy? *Journal of anatomy*, 216(2), 235–250,
- Wu, W., Cao, K., Li, C., Qian, C., Loy, C.C. (2019). Transgaga: Geometry-aware unsupervised image-to-image translation. *Proceedings of the ieee/cvf conference on computer vision and pattern recognition* (pp. 8012–8021).
- Yi, Z., Zhang, H., Tan, P., Gong, M. (2017). Dual-gan: Unsupervised dual learning for image-to-image translation. *Proceedings of the ieee international conference on computer vision* (pp. 2849–2857).
- Yu, Z., & Kovashka, A. (2020). Syntharch: Interactive image search with attribute-conditioned synthesis. *Proceedings of the ieee/cvf conference on computer vision and pattern recognition workshops* (pp. 170–171).
- Zaeemzadeh, A., Ghadar, S., Faieta, B., Lin, Z., Rahnavard, N., Shah, M., Kalarot, R. (2021). Face image retrieval with attribute manipulation. *Proceedings of the ieee/cvf international conference on computer vision* (pp. 12116–12125).
- Zhang, R., Pfister, T., Li, J. (2019). Harmonic unpaired image-to-image translation. *arXiv preprint arXiv:1902.09727*, ,
- Zhao, B., Feng, J., Wu, X., Yan, S. (2017). Memory-augmented attribute manipulation

networks for interactive fashion search. *Proceedings of the ieee conference on computer vision and pattern recognition* (pp. 1520–1528).

Zhu, J.-Y., Park, T., Isola, P., Efros, A.A. (2017). Unpaired image-to-image translation using cycle-consistent adversarial networks. *Proceedings of the ieee international conference on computer vision* (pp. 2223–2232).

Zhu, J.-Y., Zhang, R., Pathak, D., Darrell, T., Efros, A.A., Wang, O., Shechtman, E. (2017). Toward multimodal image-to-image translation. *Advances in neural information processing systems*, 30, ,